Article

Not peer-reviewed version

Effect of Rice Husk addition on the Hygrothermal, Mechanical, and Acoustic Properties of Lightened Adobe Bricks

Grégoire Banaba , Sébastien Murer , Céline Rousse , Fabien Beaumont , Christophe Bliard , Guillaume Polidori * , Eric Chatelet

Posted Date: 24 June 2025

doi: 10.20944/preprints202506.1941.v1

Keywords: adobe; lightened earth; rice husk; moisture-buffer value; compressive strength; thermal performance; acoustics

Article

Effect of Rice Husk Addition on the Hygrothermal, Mechanical, and Acoustic Properties of Lightened Adobe Bricks

Grégoire Banaba [1,2], Sébastien Murer [2], Céline Rousse [2], Fabien Beaumont [2], Christophe Bliard [3], Éric Chatelet [1] and Guillaume Polidori [2,*]

[1] Université de Technologie de Troyes, Interdisciplinary research on Society-Technology-Environment interactions (InSyTE), F-10004 Troyes, France

[2] Université de Reims Champagne-Ardenne, Institut de Thermique, Mécanique, Matériaux (ITheMM) F-51100 Reims, France

[3] Université de Reims Champagne-Ardenne, Institut de Chimie Moléculaire de Reims (ICMR), UMR 7312 CNRS, F-51100 Reims, France

* Correspondence: guillaume.polidori@univ-reims.fr

Abstract

In the context of ongoing efforts to reduce greenhouse gas emissions from the building sector, the reintegration of traditional earthen construction techniques into contemporary architectural and renovation practices presents a promising avenue. To address the inherent limitations of adobe bricks in terms of mechanical strength and water resistance, the incorporation of vegetal waste—such as rice husk—is increasingly explored. This experimental study evaluates the impact of rice husk addition on the mechanical, hygrothermal, and acoustic properties of adobe bricks. Two distinct soil types, one predominantly siliceous and the other rich in limestone, were selected and combined with 1 wt%, 2 wt%, and 3 wt% of rice husk to fabricate bio-based earthen bricks. The experimental results indicate that the influence of rice husk is strongly dependent on the mineralogical and granulometric characteristics of the soil. The most notable improvements were observed in the hygrothermal performance of the composites, particularly in terms of reduced thermal conductivity and enhanced moisture buffering capacity. From a mechanical standpoint, the benefits of rice husk incorporation were generally limited and, in some cases, detrimental, depending on the type of soil used. As for acoustic performance, the addition of rice husk did not lead to any appreciable enhancement, irrespective of the dosage applied. These findings underscore the critical role played by both the particle size distribution and chemical composition of the raw earth in optimizing the rice husk content for improving the hygrothermal, mechanical, and acoustic performance of adobe bricks.

Keywords: adobe; lightened earth; rice husk; moisture-buffer value; compressive strength; thermal performance; acoustics

1. Introduction

Earth is undoubtedly one of the oldest building materials in human history. Persian, Assyrian, Egyptian, and Babylonian civilizations made abundant use of it [1]. It is estimated that 8-10% of the world's population lives in earthen constructions, going up to 20-25% in developing countries [2]. In Europe, although largely forgotten today, earth constructions still form part of the daily landscape [1]. In France, one or more traditional earth construction techniques are found in all regions, except mountainous areas, in both rural and urban centers.

Today, the construction sector accounts for 33% of greenhouse gas emissions, 40% of material consumption, and 40% of global waste production [3]. With increasing awareness of resource depletion and the consequences of climate change over the past two decades, earth construction

 doi:10.20944/preprints202506.1941.v1

techniques have resurfaced as efficient and ecological solutions to reduce energy consumption and greenhouse gas emissions in the construction and housing sectors. However, despite its excellent carbon footprint and hygrothermal properties, raw earth remains less attractive due to its high sensitivity to water and low compressive strength compared to widespread cement-based materials. To palliate this, stabilization of earth with mineral binders such as cement or lime is often performed [4]. Unfortunately, even in small quantities, these stabilizers drastically affect the environmental cost and prevent recyclability of these materials [5]. Consequently, recent studies suggest that using organic binders from plant fibers or agricultural waste as organic reinforcement could offer a more sustainable alternative to mineral stabilizers [6–9] due to favorable physico-mechanical properties [10–12].

Rice husk, the protective layer surrounding the rice grain during growth, consists mainly of silica and organic biopolymers and represents about 20% of the rice grain's mass after harvest. It is a byproduct of rice milling, produced during the dehulling process.

Considering the potential benefits of plant waste in improving raw earth brick properties, this article focuses on the use of rice husk to enhance the hygrothermal, mechanical, and acoustic properties of adobe bricks, handmade or molded in their plastic state and air-dried [13].

Research on using raw, non-calcined rice husk in adobe manufacturing remains limited. Ouedraogo et al. [14] demonstrated that adding rice husk to a low-plasticity clay (plasticity index = 14%) enhanced compressive strength and reduced thermal conductivity. The best compressive strength (3.6 MPa) was achieved with 0.4% rice husk addition. Samson et al. [15] evaluated mechanical and physical properties of adobes with 0–2.5% rice husk by weight, noting improvements in mechanical strength and reductions in shrinkage and water absorption. Ige & Danso [16] showed that stabilizing adobes with 0.75% rice husk and 10% lime improved compressive and tensile strength by 62% and 95%, respectively. Antunes et al. [17] explored biosourced composite panels with rice husk, finding a 50% reduction in thermal conductivity and a 20% increase in humidity buffering. Buratti et al. [18] studied the thermal and acoustic performance of rice husk panels, finding thermal conductivity comparable to traditional insulation and strong sound absorption coefficients. Vatani Oskouei et al. [19] showed lower compressive and tensile strength for rice husk composites compared to palm fiber ones. Akinyele et al. [20] found that a 2% addition of 300 µm-sized rice husk particles gave the highest compressive strength (5.47 MPa) in fired clay bricks. Sutas et al. [21] compared rice husk and rice husk ash additives and found that 1% husk addition provided the best compressive strength (4 MPa), while 2% ash addition further improved properties.

The aim of the present study is to optimize the hygrothermal, mechanical, and acoustic properties of rice husk-stabilized adobes, considering the elemental composition of the earth used. The goal is to analyze formulations offering optimal mechanical strength, thermal insulation, moisture regulation, and acoustic performance, contributing to sustainable, environmentally friendly construction capable of supporting at least one story. Two soil samples from different localities will be mixed with 1, 2, and 3 wt% rice husk, and physical, mechanical, thermal, moisture, and acoustic tests will be conducted to guide the construction sector in using rice husk as an eco-friendly stabilizer for adobe production.

2. Materials and Methods

1. Geographic Origin of the Studied Soils

Two soil samples were collected from Athis and Châlons-en-Champagne, two localities in the Champagne-Ardenne region of France (Figure 1a). These two soil samples are hereafter referred to as 51-AT and 51-CH, respectively: the two digits correspond to the number of the French department, and the two letters correspond to the first two letters of the town or village from which the soils originate. Champagne-Ardenne is situated in northeastern France and constitutes a transitional region to the east of the Paris Basin. Stretching 300 km from north to south and 200 km from east to west, it covers an area of 25,600 km^2. The region is composed of Cenozoic plateaus in the west, Jurassic

 doi:10.20944/preprints202506.1941.v1

and Cretaceous plateaus in the east, and Quaternary alluvial valleys. To the north, it is bordered by the remnants of the ancient Paleozoic Ardenne mountain range. As a result, it presents a wide diversity of soil types. The Chalky Champagne, a vast chalk plain, occupies the central part of the region [22].

Figure 1. (a) Geographic origin of the soil samples - from Polidori et al. 2025 [22]; (b) 51-AT adobes collected from a traditional barn; (c) excavation site of 51-CH soil.

2. Origin of the Soil Used

Athis soil, denoted 51-AT, originates from adobes collected in the load-bearing walls of a demolished traditional barn. Their dimensions are found to be $296.3 \times 141 \times 101\ mm^3$ in average (Figure 1b, Polidori et al., 2025). Châlons soil (51-CH) is a site excavation soil (Figure 1c), collected at a depth of around 4 m below the natural soil surface.

3. Overall Characteristics of Rice Husk

The rice husk used in this study originates from the Camargue region, the heartland of French rice cultivation, which spans an area of 146,000 hectares. The rice harvesting process begins with separating the grains from the straw in the harvested sheaves, followed by the removal of impurities such as insects, minerals, and plant debris. The grains are then subjected to a drying process before undergoing dehusking. This final step separates the grain from its husks, which appear as half-shells (see Figure 2).

Rice husk accounts for approximately 20% by mass of the whole unhulled grain. In France, around 15,000 tonnes of rice husks are produced annually in the Camargue region [23]. Rice husk is composed of 70–80% organic matter (including 38% cellulose, 22% lignin, 18% pentosan, and 2% other organic substances), which is lower than most other lignocellulosic resources. The remaining 20% is primarily amorphous silica, concentrated mainly on the outer surface of the husk [24]. Rice husk is virtually rot-resistant and impervious to insect attacks.

The management of this agricultural waste includes its reuse as a fertilizer for soil enrichment, as a fuel for electricity or heat production, or as construction material in the building sector when calcined [25].

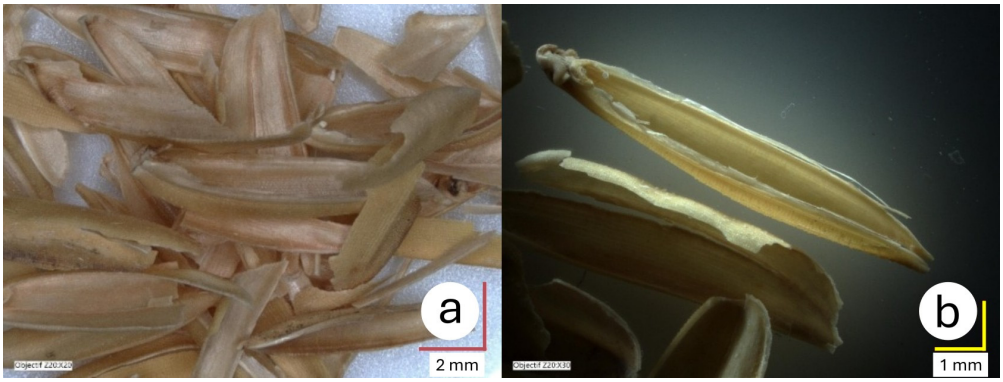

 doi:10.20944/preprints202506.1941.v1

Figure 2. Bulk rice husk (a); detail of rice husk (b).

4. Granulometry of Soil Samples

The particle size analysis was conducted in accordance with ISO 11277:2020 [26] , using wet sieving with nine sieves of decreasing mesh size ranging from 10 mm to 25 µm on randomly selected samples from each soil type.

To access particle size fractions smaller than 25 µm, laser diffraction was employed using a Malvern Mastersizer 2000 granulometer (Malvern Instruments Ltd., Worcestershire, UK). The consistency between the two granulometric techniques—one based on mass and the other on volume—is ensured by verifying that the absolute densities of the corresponding samples are comparable [22].

5. Morphology and Elemental Composition of Soil Samples and Rice Husk

The morphology and elemental chemical composition of the soil and rice husk samples were determined using a Hitachi TM3030Plus tabletop scanning electron microscope (SEM) (Hitachi High-Tech Corp, Tokyo, Japan) coupled with a Swift ES3000 energy-dispersive X-ray spectroscopy (EDXS) system. X-ray spectra were acquired at an acceleration voltage of 15 kV with an acquisition time of 300 seconds.

For scanning electron microscopy observations, the specimens were coated with a conductive Au-Pd layer via sputter coating to prevent charging effects (i.e., electron accumulation on the surface of the material), which can compromise image quality. Non-conductive samples are unable to dissipate electrical charges, resulting in image instability and inaccurate EDXS analysis. Therefore, the soil and rice husk samples were crushed and compressed into pellets for EDXS analysis. Each experiment was repeated at least three times to ensure reproducibility of the results.

To determine the size distribution of the rice husks, a set of approximately one hundred randomly selected husk samples was measured using a Keyence VHX-970F digital microscope (Keyence Corporation, Osaka, Japan). Following these measurements, a scatter plot was generated, allowing for the calculation of the average length and width of the rice husks.

6. Measurements of $CaCO_3$ and Water Contents

Decarbonization was performed using a custom-built single-unit Scheibler apparatus in accordance with the NF EN ISO 10693:1995 standard [27]. An estimation of the carbonate content in the soil samples was thus provided [22]. Moisture content was determined using a Sartorius MA100 high-precision moisture analyzer (Sartorius AG, Göttingen, Germany).

7. Adobe Manufacturing and Drying

For mechanical, hygrothermal and acoustic tests, cubic and cylindrical samples are made from each of the two soils, with rice husk contents of 1, 2 and 3 wt% (Figure 3a), then air-dried for 28 days in a controlled environment (22°C, 55 % HR), as seen in Figure 3b.

 doi:10.20944/preprints202506.1941.v1

Figure 3. Overview of the soil and rice husk volumes for a 3 wt% content (a); drying of cubic earth-rice husk samples (b).

8. Compression Tests

Given that earthen architectural design is predominantly governed by compressive stresses, compression tests were conducted using a Zwick Roell Z050 testing machine (ZwickRoell, Ulm, Germany) equipped with a 50 kN load cell. The compression rate was set at 8 mm/min in accordance with the specifications of standard NF XP P 13-901 [28], resulting in specimen failure within 1 to 2 minutes.

In this study, four adobe bricks with cubic dimensions of $100 \times 100 \times 100\ mm^3$ from each soil type, stabilized with 1%, 2%, and 3% rice husk content, were subjected to compression tests. To ensure optimal contact between the sample surfaces and the compression platens, the faces were manually smoothed using sandpaper.

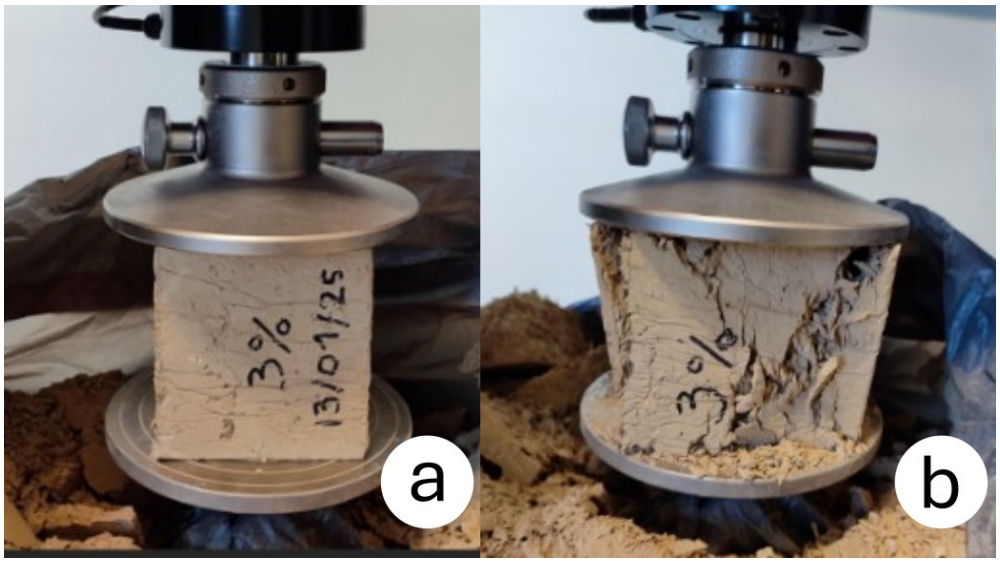

Figure 4. Compression test on a 3 wt% rice husk sample.

9. Thermal Tests

The thermal properties evaluated for both the adobe samples and the rice husk were thermal conductivity, specific heat capacity, and thermal diffusivity. The measurements were carried out using an ISOMET 2114 thermal properties analyzer (Applied Precision, Ltd., Bratislava, Slovakia). For the adobe samples, measurements were conducted based on heat flux pulses applied to the surface of the specimens. For the rice husk, a cylindrical container with dimensions $\phi 16 \times 32\ cm$ was filled and compacted to a masse of 1 kg under controlled conditions of 20.9°C and 54% relative humidity. The related thermal characteristics were determined using an API 210412 contact probe.

 doi:10.20944/preprints202506.1941.v1

10. Moisture Buffer Value (MBV)

The moisture buffering value (MBV) assesses a material's ability to regulate fluctuations in relative humidity within an enclosed space, thereby providing insight into the hygrometric comfort experienced by building occupants [22]. The MBV measurement follows the protocol described in the Nordtest project [29], which classifies moisture buffering performance from negligible to excellent. To ensure measurement reproducibility, four parallelepiped adobe samples were prepared for each soil type. Each sample measured $10 \times 10 \times 4\ cm^3$ and was sealed on the lateral and bottom surfaces using waterproof adhesive tape.

Samples were conditioned at 23°C and 50% relative humidity for 14 days and then subjected to daily RH cycles: 8 hours at 75% RH followed by 16 hours at 33% RH in a climatic chamber (Binder MKF 720, Tuttlingen, Germany). These cycles continued until the difference in mass variations measured over the last three cycles was less than 5%. The MBV value was then determined using the following equation:

$$MBV = \frac{\Delta m}{A\,(RH_{sup} - RH_{inf})} \quad (1)$$

where MBV denotes the moisture buffering value expressed in g/(m².%RH), Δm represents the mass variation during absorption and desorption, A denotes the surface area of the sample exposed to air, and RH_{sup} and RH_{inf} represent the upper (75 %) and lower (33 %) relative humidity levels, respectively.

11. Acoustic Tests

The sound absorption coefficient of the various samples was calculated over a frequency range of 125 to 4000 Hz using the impedance tube method (also known as Kundt's tube), in accordance with ISO 10534-2 [30]. To this end, 30 mm diameter samples were used for high-frequency tests (f > 2000 Hz), while 100 mm diameter samples were used for low-frequency tests (f ≤ 2000 Hz). Since material thickness influences acoustic properties, cylindrical samples with thicknesses of 30 mm and 50 mm were prepared.

3. Results and Discussion

3.1. Particle Size Distribution of Soil and Rice Husk

The particle size distribution (PSD) curves related to the two studied soils based on wet sieving and laser granulometry are presented in Figure 5.

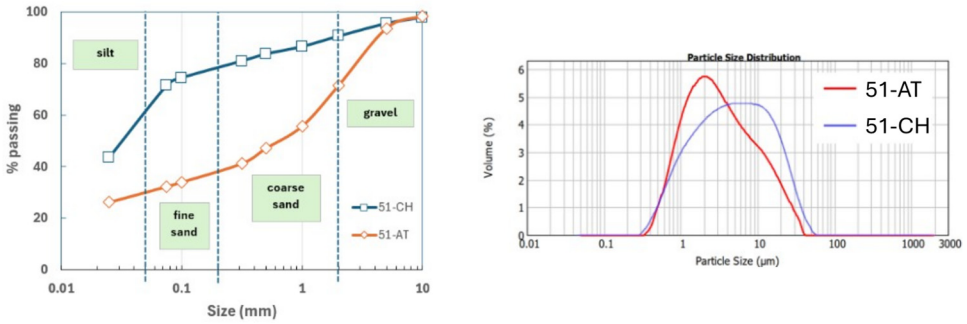

Figure 5. PSD of soil samples with wet sieving (left) and laser granulometry (right).

Typically, PSD curves in Figure 5 (left) exhibit either a bell-shaped or a sigmoidal distribution pattern in the range 25 µm – 10 mm, depending on the composition of the soils. These distinctive shapes have already been observed in a previous study [22], and are associated with the geological nature of the Champagne region (France). Gravels and stones (> 2 mm), along with coarse sands (between 0.2 and 2 mm) are predominantly present in the limestone soil of 51-AT, while minimal to

 doi:10.20944/preprints202506.1941.v1

negligible gravel content is observed in the 51-CH soil. Additionally, the residual fraction, below 25 µm, serves as a support for laser granulometry, which is widely regarded as an effective technique for estimating clay content, typically corresponding to particle sizes below 2 µm or 5 µm in common soils, depending on the classification used [5,31]. Clay content appears to be a key parameter in earth building, since clay acts as a material binder and strongly affects the mechanical properties of earth-based construction. In the present study, focused on chalky soils, laser granulometry provides an upper limit for clay content, defined as particles below 2 µm. The associated curves are depicted in Figure 5 (right).

The calculation of clay content is based on the assumption that the relative mass of fine particles (≤ 25 µm) determined by sieve analysis is equivalent to the volume fraction (%) of particles ≤ 2 µm determined by laser granulometry. This assumption is only valid if the absolute density of the soil sample is equal to that of the fine particles ≤ 25 µm. We consider this condition to be satisfied, as the differences in density are 8.54% and 0.04% for 51-AT and 51-CH, respectively. This enables the estimation of clay contents at 10.27% for 51-AT and 11.30% for 51-CH. The literature suggests that clay content in the 5-29% range is generally considered acceptable [32,33], to strike a balance between sufficient compressive strength and moderate shrinkage which may cause cracking.

Concerning rice husk as an agrowaste used to lighten the adobe bricks, Figure 6 presents a scatter plot of the rice husk average dimensions, obtained using digital microscopy over a sampling of about 100 units. A relatively homogeneous distribution in size is observed, since the mean maximum length and width are found to be 7.8 (1.5) mm and 1.8 (0.5) mm, respectively. As such, rice husk can reasonably be considered a short vegetal component.

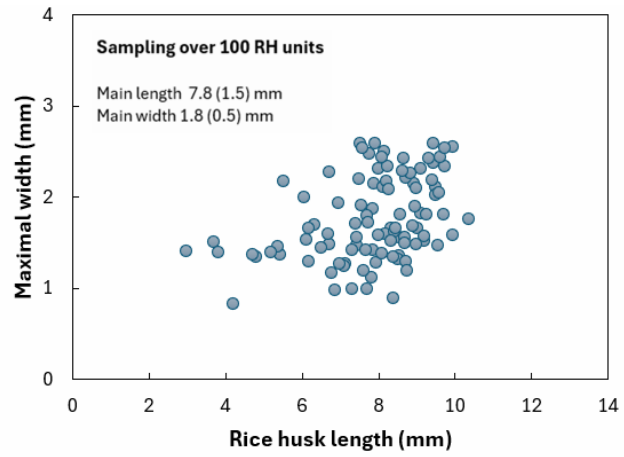

Figure 6. Size distribution of rice husk.

For comparison purposes, Chabannes et al. [25] report rice husk widths between 1 and 4 mm, and maximum lengths around 10 mm: the orders of magnitude are comparable with our results.

3.2. SEM Morphology Analysis of Soil and Rice Husk

Figures 7 and 8 present the microstructural characteristics of the two soil samples studied, obtained by scanning electron microscopy (SEM) at ×1000, ×2000, and ×5000 magnifications.

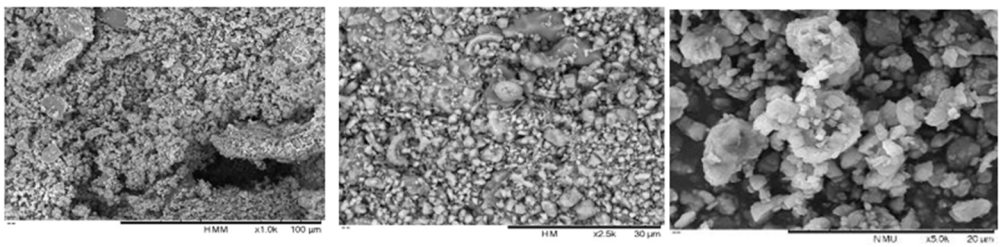

 doi:10.20944/preprints202506.1941.v1

Figure 7. SEM images of 51-AT soil (×1000, ×2500, ×5000 magnifications from left to right).

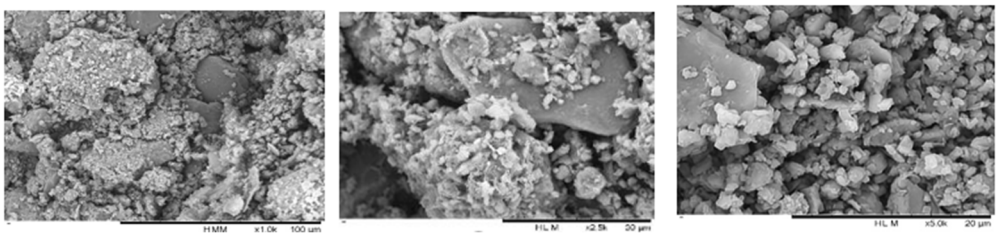

Figure 8. SEM images of 51-CH soil (×1000, ×2500, ×5000 magnifications from left to right).

In the 51-AT sample (Figure 7), a large amount of calcite micrograins is found, which is typical of limestone soils and subsoils. Coccoliths, calcitic particles produced inside the cells of unicellular marine algae known as *Coccolithophycea*, can also be observed, both whole and fragmented. Regarding the 51-CH sample (Figure 8), it appears that most of the clay content is constituted by crystalline calcite below 2 µm in size, as already reported for limestone soils [34]. More precisely, this strongly carbonated geomaterial exhibits porous aggregates of calcite nano and micrograins, where elements are in point contact or create aggregates separated by larger pores, mainly in the form of cavities.

For a closer look at the particularities of the rice husk structure, a view of the inner and outer faces is shown in Figure 9a and a cross-section in Figure 9b.

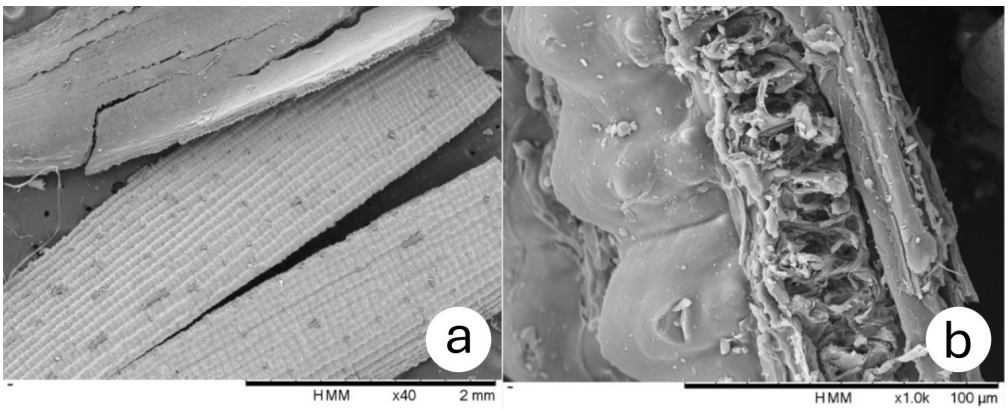

Figure 9. (a) Rice husk (×40 magnification); (b) cross-section (×1000 magnification).

Scanning electron microscopy reveals peculiarities on the outer surface of the rice husk compared to other vegetal aggregates and shows that the epidermal cells of risk husk are arranged in the shape of ridges and linear furrows, punctuated by prominent conical protuberances. Park et al. [35], as well as Do Prado & Spinacé [36], also reported these irregularities on the outer surface of the rice husk. The epidermis of the inner, concave surface is smoother than that of the outer surface [37]. The cross-section view (Figure 9b) also indicates a honeycomb structure in between the inner and outer surfaces. The presence of this air-filled layer can be assumed to result in promising thermal properties.

3.3. Elemental Chemical Composition of Soil and Rice Husk Samples

To confirm the trends observed by SEM in soils and rice husk, the elemental chemical composition of all samples was obtained by energy-dispersive X-ray spectroscopy (EDXS). Elemental spectra are presented in Figure 10.

 doi:10.20944/preprints202506.1941.v1

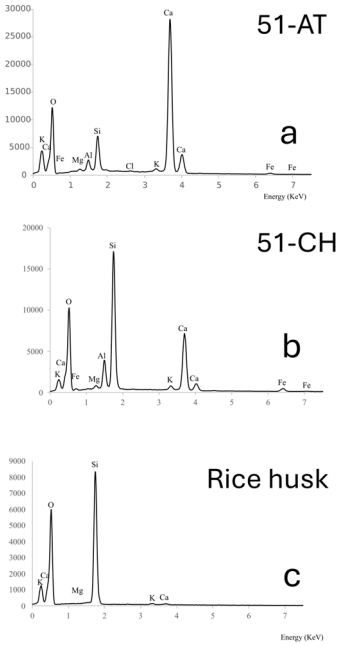

Figure 10. EDX spectra of 51-AT (a), 51-CH (b), and rice husk (c).

The analysis of EDX spectra provides a qualitative overview of the presence of elements in the different samples. For instance, calcium content is found to be higher in the 51-AT soil, compared to 51-CH. The metallic elements Fe and Al, which are present in both soils (greater content in 51-CH), are only present in trace amounts in the rice husk. Besides, although silicon is found in both soils, it clearly appears as the main mineral element observed in rice husk.

Recent studies show that metallic elements play a dominant role in the mechanical cohesion of soils. Indeed, a strong positive linear correlation (Pearson's coefficient 0.8) was observed between the peak compressive stress of soil samples and the cumulative atomic percentage of metallic elements [22] (and by extension, the metallic oxides). This phenomenon can be attributed to the propensity of metallic elements to aggregate and bond with individual soil particles within the matrix, thereby augmenting soil cohesiveness [38].

To provide quantitative information, Table 1 summarizes the elemental composition, expressed in Atomic %, deliberately limited to the main elements found in soils and rice husk samples.

Table 1. Elemental composition of soils and rice husk (Atomic %).

	O	Ca	Si	Al	Fe	K	P	Mg	Si/Ca
51-AT	71.9	21.5	3.2	0.7	0.3	0.26	-	0.32	0.15
51-CH	70.16	9.17	15.77	3.25	0.93	0.8	-	0.43	1.72
Rice husk	74.8	0.27	24.25	0.03	0.02	0.47	0.1	0.1	89.81

Results in Atomic % confirm that calcium Ca is the predominant mineral element in the 51-AT sample, with 21.5%. Besides, silicon Si is the most abundant mineral element in the 51-CH sample, associated with a significant proportion of aluminum Al and iron Fe. Consequently, the presence of metallic oxides, mainly SiO_2 and Al_2O_3 which are the main constituents of clays playing the role of cohesive binders in the manufacture of adobes, can reasonably be expected. It is found that rice husk (in its raw, unburnt form) contains approximately 24 % silicon, in line with values reported in the literature [39].

 doi:10.20944/preprints202506.1941.v1

The silicon-to-calcium ratio confirms the two soil families identified in the granulometric and morphological analyses, depending on whether this ratio is smaller than 1 (limestone soil such as 51-AT), or greater (siliceous soil such as 51-CH).

12. Physico-Chemical Characteristics of Rice Husk and Soil Samples

Soil specimens with varying rice husk contents were subjected to laboratory tests to assess their main physico-chemical characteristics, namely absolute density, dry density, porosity, moisture content, pH, % $CaCO_3$, % organic matter, and moisture buffer value. Table 2 summarizes the results for 51-AT and 51-CH soils with rice husk contents ranging from 0 to 3 wt%, along with those of rice husk alone.

Table 2. Physico-chemical properties of soils and rice husk.

	Rice husk	51-CH				51-AT			
		0 wt%	1wt%	2wt%	3wt%	0 wt%	1wt%	2wt%	3wt%
Apparent density (kg/m³)	150.9	1736.87	1714.65	1680.06	1651.43	1814.73	1763.61	1693.02	1618.90
Dry density (kg/m³)	137.6	1704.91	1687.73	1655.53	1624.19	1784.42	1748.97	1681.24	1608.48
Absolute density (kg/m³)	1284	2720.17	2705.81	2691.45	2677.09	2651.00	2637.33	2623.66	2609.99
Moisture content (%)	8.27	1.84	1.57	1.46	1.65	1.67	0.83	0.70	0.64
Porosity (%)	88.32	36.15	36.63	37.58	38.31	31.55	33.13	35.47	37.97
Clay content (%)	-	11.3	-	-	-	10.27	-	-	-
pH	6.87	7.9	-	-	-	7.7	-	-	-
$CaCO_3$ (%)	-	41.60	-	-	-	83.62	-	-	-
Organic matter (%)	-	0.24	-	-	-	1.50	-	-	-
MBV g/(m².%RH)	-	2.15	2.18	2.23	2.26	1.55	2.09	2.74	2.97

The dry density of rice husk is found at 137.6 kg/m³, in line with values reported in the literature [40]. Regarding soil samples, the average dry density values at 0 wt% rice husk content are 1814.73 kg/m³ for 51-AT and 1736.87 kg/m³ for 51-CH. These values fall within the dry density range required for adobe masonry, which, according to certain authors or standards, should vary between 14.13 and 25.07 kN/m³ [41], or between 1400 and 2200 kg/m³ [42].

The curve in Figure 11 further indicates that the dry density of adobes decreases with increasing rice husk content, with a more pronounced effect observed for 51-AT (10.8%) than for 51-CH (4.9%). This trend is consistent with the incorporation of a plant-based additive whose density is approximately 11 to 12 times lower. The variation in dry densities of the adobes falls within the range reported for earth bricks modified with plant fibers and aggregates [43]. Similar observations were made by Babé et al. [44], who reported a decrease in density and an increase in porosity for earth bricks amended with peanut shells.

 doi:10.20944/preprints202506.1941.v1

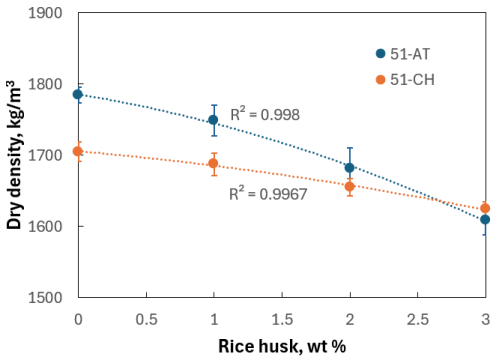

Figure 11. Dry density vs. rice husk content.

The MBV values obtained for 51-AT and 51-CH indicate that, even without the addition of rice husk, the soils can already be classified as very good to excellent moisture regulators. Since the incorporation of natural fibers increases the surface porosity of the composite—and consequently enhances its moisture buffering capacity—this classification can only improve [45,46]. To optimize time, it was deemed unnecessary to conduct MBV tests with rice husk addition.

From a chemical perspective, both soils exhibit near-neutral pH values (pH ≅ 7.8), with a slight calcareous tendency [22]. The soluble organic matter content was determined by evaporating the supernatant obtained after wet sieving and centrifugation, yielding values of 1.50% for 51-AT and 0.24% for 51-CH.

The measured calcium carbonate contents are consistent with the geological and pedological characteristics of the Champagne-Ardenne region from which the soil samples were sourced [22]. The carbonate content varies significantly, reaching 83.62% $CaCO_3$ for 51-AT and 41.60% for 51-CH. In a recent study, Polidori et al. [47] demonstrated that even a high $CaCO_3$ content of 71% in adobes can meet the structural requirements for earthen construction.

3.5. Compressive Test

Mechanical tests were carried out on cubic adobe specimens produced by mixing each type of soil with rice husk content at 1 wt%, 2 wt%, and 3 wt%. Figure 12 presents the dimensionless compressive stress, a key parameter influencing material selection in earthen construction, denoted as σ/f_c, where f_c is the peak compressive stress, plotted against the dimensionless strain $\varepsilon/\varepsilon_u$, where ε_u corresponds to the strain at peak stress f_c.

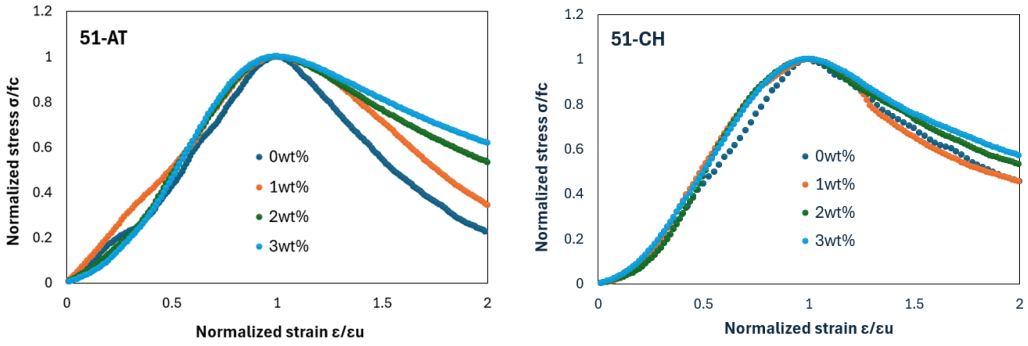

Figure 12. Normalized stress-strain curves for 51-AT (left) and 51-CH (right).

Figure 12 shows that, overall, all compression curves exhibit a similar general behavior, characterized by an initial linear elastic branch followed by a nonlinear hardening phase leading up to the peak load, after which a ductile response is observed until failure. However, a significant variation in material behavior is noted for $\varepsilon/\varepsilon_u > 1$ (i.e., beyond the peak stress point). This

 doi:10.20944/preprints202506.1941.v1

observation is consistent with findings reported by Illampas et al. [48]. The incorporation of rice husk appears to affect the ductile behavior of adobes. Although 51-AT and 51-CH raw soils display different behaviors in this regard, the addition of rice husk tends to lessen this difference. At 3% wt%, the normalized stress-strain curves are almost identical.

Table 3 summarizes the values of compressive strength of adobes as a function of rice husk content. It should be noted that the initial tangent Young's modulus E is also calculated as the slope of the curve between 0.2 and 0.8 f_c [22].

Table 3. Mechanical performance of studied soils.

	51-CH				51-AT			
	0 wt%	**1wt%**	**2wt%**	**3wt%**	**0 wt%**	**1 wt%**	**2 wt%**	**3 wt%**
Peak stress f_c (MPa)	2.57 (0.18)	2.59 (0.18)	2.18 (0.08)	1.97 (0.08)	0.52 (0.10)	0.54 (0.02)	0.53 (0.04)	0.60 (0.02)
Peak strain ε_u (%)	2.32 (0.79)	2.39 (0.60)	3.18 (0.76)	2.84 (0.67)	2.76 (0.06)	2.92 (0.33)	2.39 (0.49)	3.29 (1.16)
Mean tangent modulus E (MPa)	146.38 (44.63)	151.83 (41.85)	98.58 (17.68)	95.81 (26.08)	20.60 (5.21)	19.70 (2.84)	27.99 (6.18)	27.02 (12.06)

Figure 13 illustrates the evolution of peak compressive strength as a function of rice husk content. The two raw soils display markedly different compressive strengths (2.57 MPa for 51-CH and 0.52 MPa for 51-AT), which, as previously noted, are attributed to differences in their mineralogical compositions. For 51-CH, little variation is observed between 0 and 1 wt%, followed by a gradual decline in peak strength up to 3 wt%, reaching 1.97 MPa. In contrast, for 51-AT, the peak compressive strength increases slightly with rice husk content, reaching 0.6 MPa at 3 wt%. Nevertheless, all recorded values exceed the minimum threshold of 0.6 MPa recommended for adobe bricks used in earthen construction [28], as well as the 0.3 MPa minimum specified for earthen masonry walls [42].

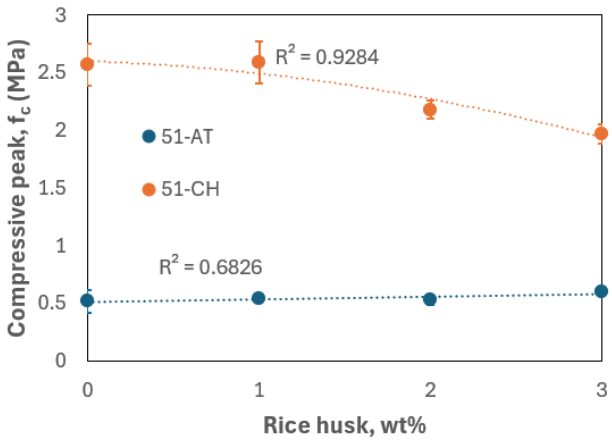

Figure 13. Compressive strength vs. rice husk content.

For both types of raw earth, compressive strength decreases at a rice husk content of 2 wt%. Similar findings were reported by Samson et al. [15] and Sutas et al. [21], who concluded that 1 wt% of rice husk was the optimal content for enhancing the compressive strength of adobe bricks. In a study on the performance of earth blocks reinforced with barley straw, Bouhicha et al. [49] clearly observed that reinforcement up to approximately 1.5 wt% improved compressive strength by 10 to 20%, depending on the soil's characteristics (plasticity index, elemental composition, particle size distribution). However, further increases in fiber content appeared to reduce the strength. Other researchers have even reported that compressive strength peaks at fiber or aggregate contents below

 doi:10.20944/preprints202506.1941.v1

1 wt% [14,16]. In the literature review by Laborel-Préneron et al. [50] on the use of plant aggregates and fibers in earthen construction, it is highlighted that the content and behavior of these materials within the soil matrix are highly variable. Some authors reported that compressive strength decreased with increasing material porosity [51], while others attributed lower compressive strength to the use of certain aggregates or fibers due to poor adhesion between the particles and the clay matrix [52,53]. Indeed, the key factor influencing the mechanical performance of these composites is the fiber-matrix adhesion. Even when the individual constituents possess favorable properties, effective fiber/matrix bonding is essential for proper load transfer within the composite [54]. According to Ouedraogo et al. [14], the strong adhesion of rice husks to the clay matrix is facilitated by their rough surface texture and high silica content. In fact, the compressive strength at 1 wt% rice husk for the clay-rich soil from Châlons is significantly higher than values reported in studies on adobes reinforced with kenaf fibers [55] or fonio straw [56]. Overall, our results are consistent with these findings in the literature.

The previous results can also be inversely corroborated by examining the dry density, as shown in Figure 14. The addition of rice husk, which contributes to the material's lightening, exerts a differing influence depending on the soil type. For 51-AT, only a marginal variation in peak compressive strength is observed as a function of density. In contrast, for 51-CH, the peak strength increases logically with rising density, reflecting the direct relationship between density and mechanical performance in this more cohesive, less carbonate-rich soil.

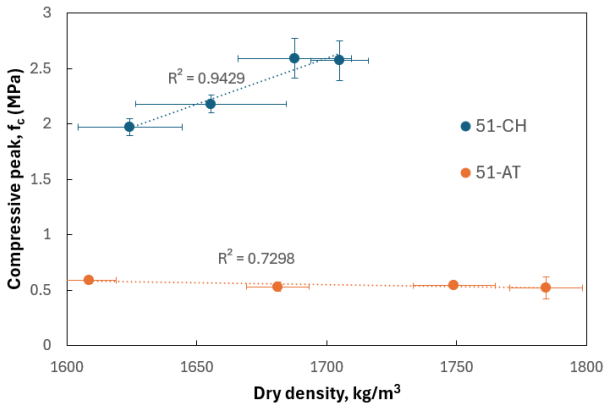

Figure 14. Compressive strength vs. dry density.

Furthermore, Table 3 shows that the tangent Young's modulus followed the same trend as the compressive strength. For sample 51-CH, the modulus decreased with increasing rice husk content, with the highest value recorded at 151.83 MPa for 1 wt% rice husk. In contrast, for sample 51-AT, the maximum Young's modulus (27.99 MPa) was achieved at 2 wt% rice husk. During compression testing, the 51-AT specimens exhibited more cracking compared to 51-CH. This may be attributed to the fact that in the 51-CH composite, rice husks form bridges with the clay matrix and are more compressible, thereby generating a higher residual strength. This phenomenon was observed during specimen failure, where loss of adhesion between the two materials was evidenced by the detachment of rice husks [50].

13. Thermal and Hydric Analyses

The results for thermal conductivity (λ), thermal diffusivity (a), and specific heat capacity (C_p) are presented in Table 4. Thermal conductivity (λ) quantifies a material's insulating capacity—the lower the conductivity, the greater the material's ability to insulate. Thermal diffusivity (a) represents a material's ability to transmit temperature variations between two surfaces; a lower diffusivity indicates slower heat transfer through the material. Specific heat capacity (C_p) characterizes the

 doi:10.20944/preprints202506.1941.v1

material's ability to store thermal energy—higher values correspond to greater heat storage capacity [57].

Table 4. Thermal characteristics of soils and rice husk.

	Rice husk	51-AT				51-CH			
		0 wt%	1wt%	2wt%	3wt%	0 wt%	1wt%	2wt%	3wt%
Thermal conductivity λ (W/m.K)	0.066 (0.001)	0.782 (0.021)	0.740 (0.045)	0.583 (0.042)	0.508 (0.034)	0.879 (0.029)	0.821 (0.015)	0.760 (0.026)	0.701 (0.022)
Diffusivity a (10^{-6} m²/s)	0.354 (0.009)	0.503 (0.030)	0.496 (0.020)	0.399 (0.029)	0.351 (0.023)	0.593 (0.031)	0.550 (0.008)	0.503 (0.014)	0.462 (0.010)
Specific heat capacity C_p (kJ/kg.K)	1.234 (0.057)	0.856 (0.033)	0.846 (0.020)	0.863 (0.014)	0.94 (0.004)	0.853 (0.015)	0.863 (0.011)	0.898 (0.009)	0.919 (0.012)

The thermal conductivity of insulation materials derived from natural fibers generally ranges between 0.03 and 0.06 W/(m.K) [58]. Rice husk is peculiar in that it is composed of a mixture of organic matter such as cellulose and lignin with high levels of insulation capabilities, and mineral components, mainly including amorphous silica, in the order of 20 % [59], which explains why rice husk displays a thermal conductivity of 0.066 W/(m·K). In contrast, earth—though superior to other conventional masonry materials—exhibits limited insulation capacity, with thermal conductivity values of 0.782 W/(m·K) and 0.879 W/(m·K) for 51-AT and 51-CH, respectively.

To evaluate the thermal impact of incorporating a bio-based insulating material into earth, Figure 15 presents the evolution of the thermal parameters of the earth–rice husk composite as a function of rice husk content, up to 3 wt%.

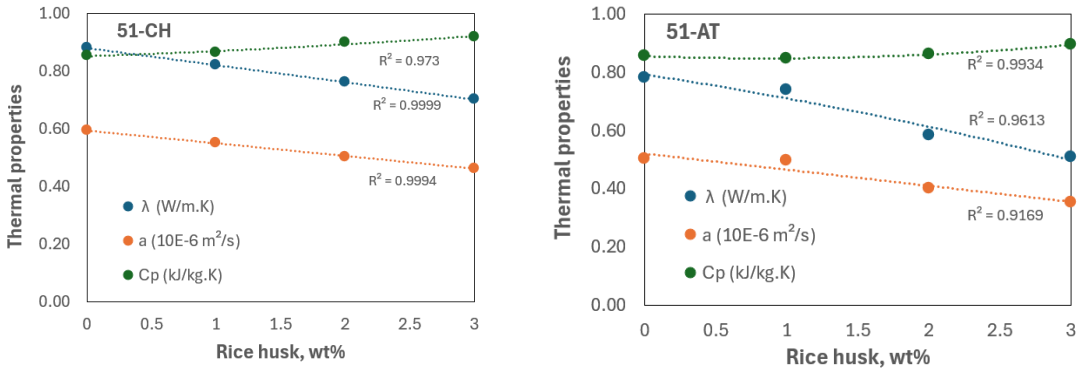

Figure 15. Thermal characteristics vs. rice husk content for 51-CH (left) and 51-AT (right).

Thermal testing results demonstrated that both the thermal conductivity (λ) and thermal diffusivity (a) of the adobes decrease monotonically with increasing rice husk content, whereas the specific heat capacity (C_p) increases as the proportion of rice husk rises in the mixture. At a concentration of 3 wt% rice husk, the thermal conductivity reached 0.508 W/(m·K) for 51-AT and 0.701 W/(m·K) for 51-CH, representing reductions of 35% and 20%, respectively, compared to the raw earth material. These outcomes reveal a substantial enhancement in the insulating performance of the adobes due to the incorporation of rice husk, as already shown by Antunes et al. [17]. This improvement in thermal conductivity can be attributed to the progressive reduction in dry density with increasing rice husk content, leading to greater porosity in the composite material, as shown in Table 2. This relationship between increased porosity and reduced thermal conductivity has also been confirmed in the literature for other bio-based composite formulations [50,60–63]. Despite low, thermal conductivity remains too high to consider adobes lightened with rice husk as excellent

 doi:10.20944/preprints202506.1941.v1

insulating materials, the threshold of which being set at 0.03 W/(m.K) by standard DIN 4108 [64]. Should this type of adobe be used as load-bearing construction material in walls, it would be necessary to further improve the insulation properties at the wall scale by creating additional insulation layers [47].

Raw earth is also valued for its high thermal inertia, which refers to its ability to delay heat transfer. Therefore, a lower thermal diffusivity indicates better resistance to temperature fluctuations. Rice husk possesses inherently better thermal properties than raw earth, with a measured diffusivity of 3.54×10^{-7} m²/s, compared to 5.03×10^{-7} m²/s for soil sample 51-AT and 5.93×10^{-7} m²/s for 51-CH. When 3 wt% rice husk is added to the raw earth, the resulting composite exhibits thermal diffusivities of 3.51×10^{-7} m²/s for 51-AT and 4.62×10^{-7} m²/s for 51-CH, corresponding to reductions of 30% and 22%, respectively. For comparison, commonly used masonry materials such as solid bricks and concrete exhibit higher diffusivities of 6.1×10^{-7} m²/s and 8.3×10^{-7} m²/s, respectively. Consequently, it can be stated that biobased earthen materials enhance the thermal comfort of the inhabitants.

Finally, the specific heat capacity of a material corresponds to the amount of energy required to raise the temperature of a unit mass by one degree Celsius. With the addition of 3 wt% rice husk, the specific heat capacity increased by 9.81% for adobe 51-AT and by 7.74% for 51-CH. These values are consistent with findings reported in previous studies [44,65,66]. In agreement with these studies, it can be inferred that the more insulating a material is, the more heat it is capable of absorbing. Accordingly, the specific heat capacity of the adobes increases as their density decreases, since plant fibers possess a higher heat capacity than mineral components [60].

Regarding the hydric properties of the studied samples, reference is made to the measurement of the moisture buffering value (MBV), which reflects a material's ability to regulate indoor humidity. This capability contributes to improved air quality, reduces microbial growth, and subsequently lowers potential risks to respiratory health. The Nordtest project [29] established a classification system for moisture buffering values, ranging from negligible to excellent, to assess a material's capacity to moderate indoor humidity. This classification is illustrated in Figure 16.

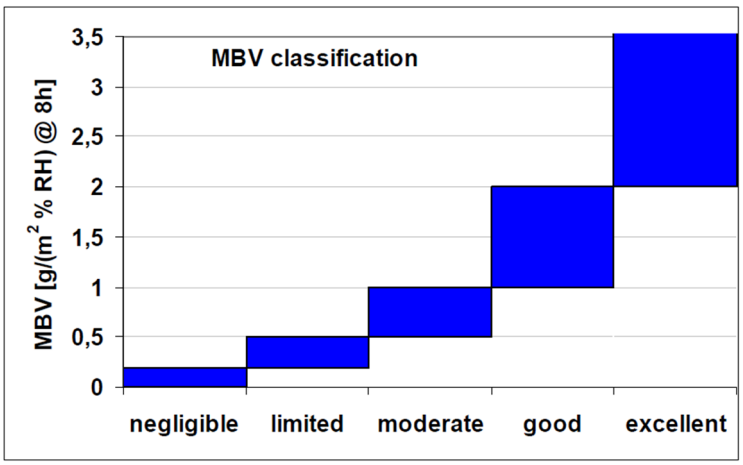

Figure 16. Classification of Moisture Buffer Values (from Rode [29]).

The values of MBV deduced from Equation (1) for all samples are summarized in Table 2 and represented as a function of rice husk content in Figure 17.

 doi:10.20944/preprints202506.1941.v1

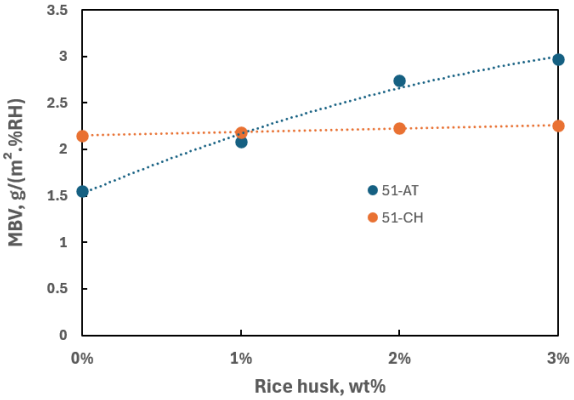

Figure 17. Moisture Buffer Value of biocomposites vs. rice husk content.

Raw calcareous 51-AT soil can be considered a good moisture regulator with MBV= 1.55 g/(m².%RH), while raw 51-CH soil appears as an excellent regulator with MBV= 2.15 g/(m².%RH). Besides, McGregor et al. [67] stipulated that the moisture performance could potentially be improved with the addition of organic aggregates. In the present study, regardless of the soil origin, an increase is observed in the moisture performance as rice husk is added in the mixture. The observations made on the 51-AT composite reveal a strong increase in MBV (+91.6%), up to 2.97 g/(m².%RH) for 3 wt% rice husk. Conversely, the MBV of siliceous 51-CH samples slightly increases (+5.1%) as rice husk content increases. Adding rice husk categorizes both composites as excellent moisture regulators. Whether strongly or slightly significant, the performance level can be assumed to be related to the elemental composition of raw soils, a siliceous soil yielding strong benefits while a calcareous one results in modest benefits. This last comment remains to be confirmed over a broader range of soil compositions.

14. Acoustic Tests

Figure 18 presents the evolution of the weighted sound absorption coefficient α_w for all adobe samples as a function of the rice husk content (wt%) in the mixture. Two different heights of cylindrical specimens, namely 30 and 50 mm, were investigated. The calculation of coefficient α_w is based on ISO 11654:1997 [68], which allows the conversion of the frequency-dependent acoustic absorption data into a single evaluation index. Annex B of the same standard provides an acoustic classification of materials according to the α_w values, ranging from "extremely absorbing" for values close to 1.0 to "reflecting" for values approaching 0.

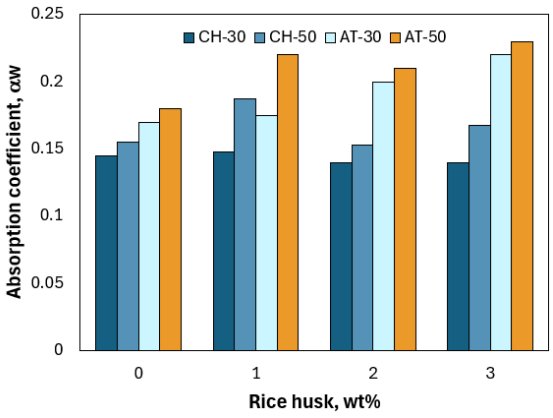

Figure 18. Weighted acoustic absorption coefficient α_w vs. rice husk content.

 doi:10.20944/preprints202506.1941.v1

The acoustic absorption coefficient varies with both the specimen thickness and the rice husk content in the mixture (Figure 18). Overall, the addition of rice husk does not significantly alter the acoustic performance of the biocomposite, which remains within a very low classification E, ranging from "hardly absorbing" to "reflecting." Indeed, for all the tests conducted, the weighted absorption coefficient was calculated to fall between 0.14 and 0.23. This result can be attributed to the condition of the surface directly exposed to sound waves: since the samples were smoothed during fabrication, they lack surface porosity and specific roughness that would otherwise contribute to sound attenuation. McGrory et al. [69] stated that a correlation exists between the thickness of the samples and the absorption coefficient values, which is also observed in both biocomposites investigated herein. However, this trend seems to only be observed for samples with limited thickness, as reported by Badouard [70], who observed that α_w no longer evolved beyond a thickness of 80 mm for samples of biocomposite formulated from grape pressing by-products.

In comparison with other commercial insulation materials, Badouard reported weighted absorption coefficient values of 0.6 for rock and glass wool (thickness: 30 mm), and 0.35 for polyurethane foam (thickness: 35 mm). It can be concluded that adobe lightened by the addition of rice husk does not offer any advantage in terms of sound absorption capabilities, with levels comparable to those of smoothed concrete.

15. Summary on the Benefits of Rice Husk Addition

Table 5 summarizes the influence of rice husk content on the Multiphysics properties of adobes. Green cells denote a beneficial gain on the performance considered, while red cells characterize a detrimental benefit.

Table 5. Synthesis of the benefits brought by rice husk addition.

	Compressive peak			Thermal conductivity			Acoustic absorption			Moisture Buffering Value		
RH, wt%	1%	2%	3%	1%	2%	3%	1%	2%	3%	1%	2%	3%
51-AT	↗	↗	↗	↘	↘	↘	→	→	→	↗	↗	↗
51-CH	↗	↘	↘	↘	↘	↘	→	→	→	→	→	→

It appears that using rice husk addition in order to lighten the material mostly affects the hygrothermal properties of the composite, namely thermal conductivity and moisture-buffering value. Mechanically speaking, the benefits are globally modest, or even detrimental depending on the raw soil used. In terms of acoustic insulation, no significant effect is observed, regardless of the ratio of natural component used.

16. Comments on Agricultural Waste Management

The world's four most widely cultivated crops—sugarcane, maize, cereals, and rice—generate substantial quantities of agricultural waste, the management of which presents global challenges. Rice husk may be marginally used in its unburnt current state (gardening mulch, animal bedding), but is mainly randomly burnt for crop drying, energy production, and biochar [71]. In regions with high rice production, the open burning of rice residues remains prevalent, significantly contributing to air pollution and posing serious risks to both human health and the environment. This practice leads to the release of greenhouse gases (GHGs), notably carbon dioxide (CO_2), nitrous oxide (N_2O), and methane (CH_4).

To assess the environmental relevance of incorporating rice husk into construction materials (excluding insulation applications), it is useful to estimate the potential volumes involved. In France, annual rice husk production is estimated at 65,000 tonnes [72], corresponding to approximately 6.5 m^3 per hectare. In the present study, up to 3 wt% of rice husk was incorporated into the raw earth adobe formulations, which equates to 27.1 vol% for 51-AT and 26.3 vol% for 51-CH, calculated using the following equation:

 doi:10.20944/preprints202506.1941.v1

$$vol\% = \frac{100}{1+\left(\frac{100}{wt\%}-1\right)\frac{\rho_h}{\rho_{soil}}}, \quad (2)$$

where ρ_h and ρ_{soil} denote the bulk densities of rice husk and soil, respectively.

Consider a single-story house of 120 m² with 3-meter-high walls and a wall thickness of 30 cm constructed from earth adobes lightened with rice husk. A rough estimate, based on the aforementioned volumetric fractions, suggests that approximately 21 m³ of rice husk would be required, corresponding to about 3.171 tonnes. Given that the calcination yield of rice husk is approximately 20%, and that each kilogram of rice husk ash generates 1.72 kg of CO_2 equivalent [73], it can be inferred that for the aforementioned dwelling, incorporating rice husk into earthen construction materials rather than open-air incineration would prevent the emission of approximately 1,090 kg of CO_2eq into the atmosphere. Extrapolated to a larger scale, utilizing rice husk as a construction material rather than burning it—which remains the predominant practice in major rice-producing countries—could result in a significantly reduced environmental footprint.

4. Conclusions

This study investigated the potential of rice husk as a bio-based additive for improving the performance of adobe bricks, focusing on mechanical, hygrothermal, and acoustic properties, by incorporating 1, 2, and 3 wt% of rice husk into two distinct soil types—one siliceous (51-CH) and one calcareous (51-AT).

From a mechanical perspective, the addition of rice husk had varying effects depending on soil type. For 51-CH, a siliceous soil rich in metallic oxides, the compressive strength peaked at 1 wt% rice husk, indicating improved mechanical cohesion and optimal fiber-matrix interaction at low content. Conversely, for 51-AT, a calcareous soil with higher carbonate content, the compressive strength remained relatively low but slightly improved at 3 wt%, likely due to increased ductility and porosity. Overall, the compressive strengths remained above the thresholds recommended for earthen construction.

Thermal analyses revealed a consistent trend: as the rice husk content increased, thermal conductivity and diffusivity decreased while specific heat capacity increased. These changes indicate improved insulation and thermal inertia, attributed primarily to the low density and high porosity induced by rice husk incorporation. At 3 wt%, reductions in thermal conductivity reached up to 35% for 51-AT and 20% for 51-CH, reflecting significant thermal performance enhancement.

Moisture buffering performance was already high for both raw soils, ranging from good (raw 51-AT soil) to excellent (all compositions), and the known effect of increased surface porosity with fiber addition suggests even greater moisture regulation potential with rice husk inclusion. However, acoustic tests showed minimal improvement, with sound absorption coefficients remaining low across all samples due to the smooth surface finish and limited macro-porosity.

Beyond the material performance, the environmental dimension of this study highlighted the value of utilizing agricultural waste—such as rice husk—in construction to reduce greenhouse gas emissions. Avoiding open-air burning of rice residues through their incorporation into adobe bricks could significantly cut CO_2 emissions, presenting a compelling case for circular and low-impact building practices.

Overall, rice husk appears to be a promising bio-based stabilizer for earthen construction, especially from a hygrothermal viewpoint, with optimal content dependent on soil properties and targeted performance criteria.

Author Contributions: All authors have read and agreed to the published version of the manuscript.

Funding: This research received no external funding.

Institutional Review Board Statement: Not applicable.

Informed Consent Statement: Not applicable

 doi:10.20944/preprints202506.1941.v1

Data Availability Statement: Data will be made available upon request.

Acknowledgments: During the preparation of this manuscript, the author used ChatGPT 4-turbo for grammatical improvement purposes. The authors have reviewed and edited the output and take full responsibility for the content of this publication.

Conflicts of Interest: The authors declare no conflicts of interest.

References

1. Doat P, Hays A, Houben H, Matuk S, Vitoux F. Construire en Terre. Parenthèses, editor. 1979.
2. Marsh ATM, Kulshreshtha Y. The state of earthen housing worldwide: how development affects attitudes and adoption. Building Research & Information. 2022 Jul 4;50(5):485–501.
3. Ness DA, Xing K. Toward a Resource-Efficient Built Environment: A Literature Review and Conceptual Model. J Ind Ecol [Internet]. 2017 Jun 1 [cited 2025 Apr 29];21(3):572–92. Available from: https://onlinelibrary.wiley.com/doi/full/10.1111/jiec.12586
4. Danso H, Martinson DB, Ali M, Williams JB. Physical, mechanical and durability properties of soil building blocks reinforced with natural fibres. Constr Build Mater. 2015 Dec 30;101:797–809.
5. Van Damme H, Houben H. Earth concrete. Stabilization revisited. Cem Concr Res. 2018 Dec 1;114:90–102.
6. Vissac A, Bourgès A, Gandreau D, Anger R, Fontaine L. argiles & biopolymères - les stabilisants naturels pour la construction en terre. Villefontaine; 2017.
7. Amziane S, Sonebi M. Overview on Biobased Building Material made with plant aggregate. RILEM Technical Letters [Internet]. 2016 Jun 2 [cited 2025 Apr 28];1:31–8. Available from: https://letters.rilem.net/index.php/rilem/article/view/9
8. Peñaloza D. The role of biobased building materials in the climate impacts of construction. [Stockholm]: KTH Royal Institute of Technology; 2017.
9. Arduin D, Caldas LR, Claro CC, Rocha F, Andrejkovicová S. Comparative study on stabilized oyster shells adobes: Mechanical resistance, durability and GHG emissions assessment. Lourenço PB, Azenha M, Pereira JM, editors. MATEC Web of Conferences [Internet]. 2024 Sep 16;403:06001. Available from: https://www.matec-conferences.org/10.1051/matecconf/202440306001
10. Mohajerani A, Hui SQ, Mirzababaei M, Arulrajah A, Horpibulsuk S, Kadir AA, et al. Amazing Types, Properties, and Applications of Fibres in Construction Materials. Materials 2019, Vol 12, Page 2513 [Internet]. 2019 Aug 7 [cited 2025 Apr 29];12(16):2513. Available from: https://www.mdpi.com/1996-1944/12/16/2513/htm
11. Lagouin M, Magniont C, Sénéchal P, Moonen P, Aubert JE, Laborel-préneron A. Influence of types of binder and plant aggregates on hygrothermal and mechanical properties of vegetal concretes. Constr Build Mater. 2019 Oct 20;222:852–71.
12. Paul SC, Mbewe PBK, Kong SY, Šavija B. Agricultural Solid Waste as Source of Supplementary Cementitious Materials in Developing Countries. Materials 2019, Vol 12, Page 1112 [Internet]. 2019 Apr 3 [cited 2025 Apr 29];12(7):1112. Available from: https://www.mdpi.com/1996-1944/12/7/1112/htm
13. Anger R. Approche granulaire et colloïdale du matériau terre pour la construction. [Lyon]: INSA; 2011.
14. Ouedraogo M, Bamogo H, Sanou I, Dao K, Ouedraogo KAJ, Aubert JE, et al. Microstructure, Physical and Mechanical Properties of Adobes Stabilized with Rice Husks. International Journal of Architectural Heritage [Internet]. 2023 Aug 3 [cited 2025 Apr 29];17(8):1348–63. Available from: https://www.tandfonline.com/doi/abs/10.1080/15583058.2022.2034072
15. Samson M, Edgar NG, Tikri B, Akana TF, Bobet O, Samson M, et al. Thermal Characteristics of Earth Blocks Stabilized by Rice Husks. Open Journal of Applied Sciences [Internet]. 2023 Oct 17 [cited 2025 Apr 29];13(10):1796–819. Available from: https://www.scirp.org/journal/paperinformation?paperid=128679
16. Ige O, Danso H. Experimental Characterization of Adobe Bricks Stabilized with Rice Husk and Lime for Sustainable Construction. Journal of Materials in Civil Engineering [Internet]. 2021 Nov 17 [cited 2025 Apr 28];34(2):04021420. Available from: https://ascelibrary.org/doi/abs/10.1061/%28ASCE%29MT.1943-5533.0004059

 doi:10.20944/preprints202506.1941.v1

17. Antunes A, Faria P, Silva V, Brás A. Rice husk-earth based composites: A novel bio-based panel for buildings refurbishment. Constr Build Mater. 2019 Oct 10;221:99–108.
18. Buratti C, Belloni E, Lascaro E, Merli F, Ricciardi P. Rice husk panels for building applications: Thermal, acoustic and environmental characterization and comparison with other innovative recycled waste materials. Constr Build Mater. 2018 May 20;171:338–49.
19. Vatani Oskouei A, Afzali M, Madadipour M. Experimental investigation on mud bricks reinforced with natural additives under compressive and tensile tests. Constr Build Mater. 2017 Jul 1;142:137–47.
20. Akinyele J, Olateju O, Oikelome O. Rice Husk as Filler in the Production of Bricks Using Gboko Clay. Nigerian Journal of Technology [Internet]. 2015 Sep 21 [cited 2025 Apr 28];34(4):672–8. Available from: https://www.ajol.info/index.php/njt/article/view/124029
21. Sutas J, Mana A, Pitak L. Effect of Rice Husk and Rice Husk Ash to Properties of Bricks. Procedia Eng. 2012 Jan 1;32:1061–7.
22. Polidori G, Aras-Gaudry A, Rousse C, Beaumont F, Bogard F, Murer S, et al. Analysis of adobes from vernacular raw earth buildings in the Champagne region (France). Constr Build Mater. 2025 Apr 4;470:140582.
23. Chabannes M. Formulation et étude des propriétés mécaniques d'agrobétons légers isolants à base de balles de riz et de chènevotte pour l'éco-construction. [Montpellier]: Université de Montpellier; 2015.
24. Johar N, Ahmad I, Dufresne A. Extraction, preparation and characterization of cellulose fibres and nanocrystals from rice husk. Ind Crops Prod. 2012 May 1;37(1):93–9.
25. Chabannes M, Bénézet JC, Clerc L, Garcia-Diaz E. Use of raw rice husk as natural aggregate in a lightweight insulating concrete: An innovative application. Constr Build Mater. 2014 Nov 15;70:428–38.
26. AFNOR. NF EN ISO 11277:2020 Qualité du sol — Détermination de la répartition granulométrique de la matière minérale des sols — Méthode par tamisage et sédimentation. 2020.
27. AFNOR. NF EN ISO 10693 :1995. Qualité du sol - Détermination de la teneur en carbonate - Méthode volumétrique. 1995.
28. AFNOR. XP P13-901:2022 Blocs de terre comprimée pour murs et cloisons : définitions - Spécifications - Méthodes d'essais - Conditions de réception. 2022.
29. Rode C;, Peuhkuri RH, Hansen KK, Time B;, Svennberg K;, Arfvidsson J;, et al. NORDTEST Project on Moisture Buffer Value of Materials. In: AIVC 26th conference: Ventilation in relation to the energy performance of buildings Air Infiltration and Ventilation. APA; 2005. p. 47–52.
30. AFNOR. ISO 10534-2:2023 - Acoustique — Détermination des propriétés acoustiques aux tubes d'impédance — Partie 2: Méthode à deux microphones pour le coefficient d'absorption sonore normal et l'impédance de surface normale [Internet]. 2023 [cited 2025 Apr 30]. Available from: https://www.iso.org/fr/standard/81294.html
31. Garcia-Gaines RA, Frankenstein S. USCS and the USDA Soil Classification System: Development of a Mapping Scheme [Internet]. 2015 Mar [cited 2024 Dec 4]. Available from: https://apps.dtic.mil/sti/citations/tr/ADA614144
32. Abhilash HN, Hamard E, Beckett CTS, Morel JC, Varum H, Silveira D, et al. Mechanical Behaviour of Earth Building Materials. In: Fabbri A, Morel JC, Aubert JE, Bui QB, Gallipoli D, Reddy BVV, editors. Testing and Characterisation of Earth-based Building Materials and Elements: State-of-the-Art Report of the RILEM TC 274-TCE. Cham: Springer International Publishing; 2022. p. 127–80.
33. Jiménez Delgado MC, Guerrero IC. The selection of soils for unstabilised earth building: A normative review. Constr Build Mater. 2007 Feb 1;21(2):237–51.
34. Kerry R, Rawlins BG, Oliver MA, Lacinska AM. Problems with determining the particle size distribution of chalk soil and some of their implications. Geoderma. 2009 Sep 15;152(3–4):324–37.
35. Park BD, Gon Wi S, Ho Lee K, Singh AP, Yoon TH, Soo Kim Y. Characterization of anatomical features and silica distribution in rice husk using microscopic and micro-analytical techniques. Biomass Bioenergy. 2003 Sep 1;25(3):319–27.
36. Do Prado KDS, Spinacé MADS. Characterization of Fibers from Pineapple's Crown, Rice Husks and Cotton Textile Residues. Materials Research [Internet]. 2015 May 1 [cited 2025 Apr 28];18(3):530–7. Available from: https://www.scielo.br/j/mr/a/rsZmR93NTJB6BPzmnBYvwKB/abstract/?lang=en

 doi:10.20944/preprints202506.1941.v1

37. Jauberthie R, Rendell F, Tamba S, Cisse I. Origin of the pozzolanic effect of rice husks. Constr Build Mater. 2000 Dec 1;14(8):419–23.
38. Walter L, Medjigbodo G, Claudot L, Nait-Rabah O, Linguet L. Influence of metal oxides and particle size on earthen mortar built with tropical soils. Academic Journal of Civil Engineering. 2022;40(2):1–10.
39. Hamidu I, Afotey B, Kwakye-Awuah B, Anang DA. Synthesis of silica and silicon from rice husk feedstock: A review. Heliyon. 2025 Feb 28;11(4):e42491.
40. Luh BS. Rice. Vol. 2. Springer Science & Business Media; 1991.
41. Sánchez A, Varum H, Martins T, Fernández J. Mechanical properties of adobe masonry for the rehabilitation of buildings. Constr Build Mater. 2022 May 23;333:127330.
42. Confédération de la construction en terre crue. Guide des bonnes pratiques de la construction en terre crue. 2020 Oct.
43. Bobet O, Seynou M, Zerbo L, Bamogo H, Sanou I, Sawadogo M. Propriétés mécanique, hydrique et thermique de briques en terre crue amendées aux coques d'arachide. J Soc Ouest-Afr Chim [Internet]. 2020 [cited 2025 Apr 28]; Available from: http://www.soachim.orgJ.Soc.Ouest-Afr.Chim.
44. Babé C, Kidmo DK, Tom A, Mvondo RRN, Boum RBE, Djongyang N. Thermomechanical characterization and durability of adobes reinforced with millet waste fibers (sorghum bicolor). Case Studies in Construction Materials. 2020 Dec 1;13:e00422.
45. Zouaoui Y, Benmahiddine F, Yahia A, Belarbi R. Hygrothermal and Mechanical Behaviors of Fiber Mortar: Comparative Study between Palm and Hemp Fibers. Energies 2021, Vol 14, Page 7110 [Internet]. 2021 Nov 1 [cited 2025 May 27];14(21):7110. Available from: https://www.mdpi.com/1996-1073/14/21/7110/htm
46. Niang I, Maalouf C, Moussa T, Bliard C, Samin E, Thomachot-Schneider C, et al. Hygrothermal performance of various Typha–clay composite. J Build Phys [Internet]. 2018 Apr 17 [cited 2025 May 27];42(3):316–35. Available from: https://hal.science/hal-02068214
47. Polidori G, Aras-Gaudry A, Beaumont F, Bogard F, Murer S, Lachi M, et al. Adobe Bricks of the Champagne Region (France): Characterization of a Chalky Raw Earth Construction Material. Materials 2024, Vol 17, Page 2307. 2024 May 13;17(10):2307.
48. Illampas R, Ioannou I, Charmpis DC. Adobe bricks under compression: Experimental investigation and derivation of stress–strain equation. Constr Build Mater. 2014 Feb 28;53:83–90.
49. Bouhicha M, Aouissi F, Kenai S. Performance of composite soil reinforced with barley straw. Cem Concr Compos. 2005 May 1;27(5):617–21.
50. Laborel-Préneron A, Aubert JE, Magniont C, Tribout C, Bertron A. Plant aggregates and fibers in earth construction materials: A review. Constr Build Mater. 2016 May 15;111:719–34.
51. Bouguerra A, Ledhem A, De Barquin F, Dheilly RM, Quéneudec M. Effect of microstructure on the mechanical and thermal properties of lightweight concrete prepared from clay, cement, and wood aggregates. Cem Concr Res. 1998 Aug 1;28(8):1179–90.
52. Quagliarini E, Lenci S. The influence of natural stabilizers and natural fibres on the mechanical properties of ancient Roman adobe bricks. J Cult Herit. 2010 Jul 1;11(3):309–14.
53. Khedari J, Watsanasathaporn P, Hirunlabh J. Development of fibre-based soil–cement block with low thermal conductivity. Cem Concr Compos. 2005 Jan 1;27(1):111–6.
54. Lahouioui M. Élaboration et évaluation des propriétés physico-thermiques et acoustiques de nouveaux éco-composites à base de bois de palmier. [Gabès]: Université de Gabès; 2019.
55. Ouedraogo M, Dao K, Millogo Y, Seynou M, Aubert JE, Gomina M. Influence des fibres de kenaf (Hibiscus altissima) sur les propriétés physiques et mécaniques des adobes. Journal de la Société Ouest-Africaine de Chimie. 2017;43:63.
56. Ouedraogo M, Dao K, Millogo Y, Aubert JE, Messan A, Seynou M, et al. Physical, thermal and mechanical properties of adobes stabilized with fonio (Digitaria exilis) straw. Journal of Building Engineering. 2019 May 1;23:250–8.
57. Marwa LAHOUIOUI. Elaboration et évaluation des propriétés physico-thermiques et acoustiques de nouveaux éco-composites à base de bois de palmier. 2019 Oct.
58. Hung Anh LD, Pásztory Z. An overview of factors influencing thermal conductivity of building insulation materials. Journal of Building Engineering. 2021 Dec 1;44:102604.

 doi:10.20944/preprints202506.1941.v1

59. Nzereogu PU, Omah AD, Ezema FI, Iwuoha EI, Nwanya AC. Silica extraction from rice husk: Comprehensive review and applications. Hybrid Advances. 2023 Dec 1;4:100111.
60. Modjonda S, Etienne Y, Raidandi D. Thermal and Mechanical Characterization of Compressed Clay Bricks Reinforced by Rice Husks for Optimizing Building in Sahelian Zone. Advances in Materials Physics and Chemistry. 2023 Oct 30;13(10):177–96.
61. Al Rim K, Ledhem A, Douzane O, Dheilly RM, Queneudec M. Influence of the proportion of wood on the thermal and mechanical performances of clay-cement-wood composites. Cem Concr Compos. 1999 Aug 1;21(4):269–76.
62. Ledhem A, Dheilly RM, Benmalek ML, Quéneudec M. Properties of wood-based composites formulated with aggregate industry waste. Constr Build Mater. 2000 Sep 1;14(6–7):341–50.
63. Millogo Y, Morel JC, Aubert JE, Ghavami K. Experimental analysis of Pressed Adobe Blocks reinforced with Hibiscus cannabinus fibers. Constr Build Mater. 2014 Feb 15;52:71–8.
64. Standard DIN 4108 - Thermal insulation and energy economy in buildings [Internet]. Berlin; 2024 Jan [cited 2024 Apr 4]. Available from: https://www.boutique.afnor.org/en-gb/standard/din-41084/thermal-insulation-and-energy-economy-in-buildings-part-4-hygrothermal-desi/eu167388/261822
65. Demir I. Effect of organic residues addition on the technological properties of clay bricks. Waste Management. 2008 Jan 1;28(3):622–7.
66. Delot P. Balle de riz - Compilation d'éléments techniques en vue de son utilisation en isolation thermique [Internet]. 2015 [cited 2025 Apr 29]. Available from: www.ballederiz.fr
67. McGregor F, Heath A, Maskell D, Fabbri A, Morel JC. A review on the buffering capacity of earth building materials. Proceedings of the Institution of Civil Engineers - Construction Materials. 2016 Jan 12;169(5):241–51.
68. AFNOR. NF EN ISO 11654:1997 Acoustique - Absorbants pour l'utilisation dans les bâtiments - Évaluation de l'absorption acoustique. 1997.
69. Mcgrory M, Castro Cirac D, Gaussen O, Cabrera D. Sound absorption coefficient measurement: Re-examining the relationship between impedance tube and reverberant room methods. In: Proceedings of Acoustics 2012. Fremantle: Australian Acoustical Society; 2012.
70. Badouard C. Valorisation des sous-produits de pressurage du raisin : caractérisation thermomécanique d'un nouveau matériau biosourcé à base d'aignes. [Reims]: Université de Reims Champagne-Ardenne; 2023.
71. Koul B, Yakoob M, Shah MP. Agricultural waste management strategies for environmental sustainability. Environ Res. 2022 Apr 15;206:112285.
72. Delot P, Association Bâtir en balles. Balle de riz de Camargue. 2017.
73. Datchossa AT, Doko VK, Houanou KA, Olodo EET. 2022 Study of the ecological interest of a rice husk ash mortar. Aust J Basic Appl Sci [Internet]. 2022;16(12):8–16. Available from: www.ajbasweb.com